Front. Optoelectron. China 2011, 4(4): 369–377
DOI 10.1007/s12200-011-0181-6

RESEARCH ARTICLE

Application of Poly (3, 4-ethylenedioxythiophene): polystyrenesulfonate counter electrode in polymer heterojunction dye-sensitized solar cells

Gentian YUE, Jihuai WU (✉), Jianming LIN, Miaoliang HUANG, Ying YAO, Leqing FAN, Yaoming XIAO

Engineering Research Center of Environment-Friendly Functional Materials, Ministry of Education, The Key Laboratory for Functional Materials of Fujian Higher Education, Institute of Material Physical Chemistry, Huaqiao University, Quanzhou 362021, China

Abstract A Poly (3, 4-ethylenedioxythiophene): polystyrenesulfonate (PEDOT:PSS)/carbon conductive paste was prepared and coated on a conducting FTO glass to construct counter electrode for polymer heterojunction dye-sensitized solar cells (DSSCs). The surface morphology, conductivity, sheet resistance, redox properties and photoelectric properties of carbon electrode were observed respectively by scanning electron microscopy, four-probe tester and CHI660D electrochemical measurement system. The experimental results showed that DSSCs had the best photoelectric properties for PEDOT:PSS/carbon counter electrode annealing at 80°C in vacuum conditions. Using [6, 6]-phenyl-C_{61}-butyric acid methyl ester (PCBM)/poly (3-hexylthiophene) (P3HT) heterojunction to replace I_3^-/I^- redox electrolyte, the overall energy conversion efficiency of the DSSCs with barrier layer reached 4.11% under irradiation of a simulated solar light with a intensity of 100 $mW \cdot cm^{-1}$ (AM 1.5), which is higher 20% than that of the DSSCs with Pt counter electrode (3.42%). The excellent photoelectric properties, simple preparation procedure and low cost allow the PEDOT:PSS/carbon electrode to be a credible alternative used in DSSCs.

Keywords Poly (3, 4-ethylenedioxythiophene): polystyrenesulfonate (PEDOT:PSS), counter electrode, polymer heterojunction, dye-sensitized solar cell (DSSC), photoelectric properties

1 Introduction

The sun is the largest carbon-neutral energy source that has not been fully utilized. Although solar cell devices have existed based on inorganic semiconductor to efficiently harvest solar energy, the cost of these conventional devices is too high and pollution to the environment. This is the major motivation for the research of Grätzel solar cell in 1991 [1], organic photovoltaic (OPV) materials and bulk heterojunction solar cells [2,3]. Gratzel solar cells have higher conversion efficiency [4–6] which has aroused intensive interest over the past decade due to its low cost and clean energy conversion devices [7–9]. In general, the dye-sensitized solar cells (DSSCs) consists of a sandwich structure with a dye-sensitized porous nanocrystalline TiO_2 film electrode for absorbing visible light, a redox electrolyte, and a platinized counter electrode to collect electrons and catalyze I_2/I^- redox-coupled regeneration reaction in electrolyte. Platinum as a conventional counter-electrode material in the devices is a burden for large-scale applications of DSSCs because it is one of the most expensive materials available [10,11]. So, the key challenges for DSSCs are developing low-cost and platinum-free counter-electrode materials with relatively high conversion efficiency. However, highly desired counter-electrode materials of high electrical conductivity and superior electrocatalytic activity [12,13] are rare.

Recently, to reduce the production cost of solar devices, a lot of carbon materials are researched to replace platinum electrode [14–18] and got a good performance with carbon materials. However, there is an intrinsic problem of insolubility in most solvents and many groups have tried to solve it in decades [19,20]. And there are few reports about using conducting polymers and carbon materials hybrid as counter electrode materials in DSSCs. In contrast, the polymer grafting onto carbon materials can improve the solubility of carbon materials without the conductivity loss and the conductivity of the film can be further improved in combination with highly conductive [21,22].

Received August 18, 2011; accepted September 22, 2011

E-mail: jhwu@hqu.edu.cn (J. Wu)

Polymer poly (3, 4–ethylenedioxythiophene): poly (styrenesulfonate) (PEDOT:PSS) as a good charge transfer polymer material with its transparent, good conductivity (0.1 to 1 × 10^5 S/cm) and solubility in polar solvent has been extensively researched [22–24]. Of course, PEDOT: PSS is the potent candidate studied on the application of carbon materials and prepared PEDOT:PSS/carbon composite films as an electrode of DSSCs.

In this work, PEDOT: PSS/carbon conductive paste was coated on a conducting FTO glass to construct PEDOT: PSS/carbon counter electrode with the vacuum low temperature annealed at 80°C, which based on the adhesion, transparent and high conductivity of PEDOT: PSS, added the cheap graphite powder and carbon black, dimethyl sulfoxide, polyethylene Glycol 400 and a small amount of polyvinylpyrrolidone prepared. We researched a series of performances about the surface morphology, conductivity, sheet resistance, redox properties and photoelectric properties of PEDOT:PSS/carbon electrode, Using [6, 6]-phenyl-C_{61}-butyric acid methyl ester (PCBM)/poly (3-hexylthiophene) (P3HT) heterojunction to replace I_3^-/I^- redox electrolyte. It is expected that photoelectric performance of the DSSCs with PEDOT:PSS/carbon electrode can be improved.

2 Experimental

2.1 Materials

P3HT (purity 99.995%) and PCBM (purity 99.995%) were purchased from Luoyang Microlight Material Technology Co., Ltd, China. PEDOT:PSS (pH = 2.1, surface resistance = 1×10^5–3×10^5 Ω/sq) come from Shanghai Chunyuan Phytochemistry Co., Ltd., China. The organometallic compound sensitized dye N-719 [$RuL_2(NCS)_2$, L = 4,4′-dicarboxylate-2,2′-bipyridine] was obtained from Solaronix SA (Switzerland). 1,2-dichlorobenzene (CB), anhydrous ethanol (ETOH), isopropanol, nitric acid (HNO_3), acetic acid (HAc), DMSO, graphite, carbon black, PVP, Polyethylene glycol with average molecular weight 20000 and 400 (PEG-20000 and PEG-400) and OP emulsification agent (Triton X-100), tetrabutyltitanate [$Ti(OBu)_4$] and titanium tetrachloride ($TiCl_4$) were analytic grade purity and purchased from Shanghai Chemical Agent Ltd., China. All reagents were used without further treatment before using.

Conductive glass plate (FTO glass, Fluorine doped tin oxide over-layer, sheet resistance 8 Ω/sq, purchased from Hartford Glass Co., USA) was used as a substrate for precipitating TiO_2 porous film and was cut into 1 cm× 2 cm sheets.

2.2 Preparation of dye-sensitized TiO_2 films

TiO_2 nanoporous film was prepared by following procedure [3,4]. Tetrabutyltitanate (10 mL) was rapidly added to distilled water (100 mL) and a white precipitate was formed immediately. The precipitate was filtered using a glass frit and washed with distilled water. Under vigorous stirring, the filter cake was added to 1 mL nitric acid and 10 mL acetic acid aqueous solution (150 mL) at 80°C until the slurry became a translucent blue-white liquid. The blue-white liquid was autoclaved at 200°C for 12 h to form milky white slurry. The resultant slurry was concentrated to 1/4 of its original volume, then PEG-20000 (10 wt.% slurry) and a few drops of emulsification regent of Triton X-100 was added to form a TiO_2 colloid.

A conductive glass sheet (FTO) was immersed in an isopropanol solution for 48 h to remove surface impurities. Then it was cleaned in Triton X-100 aqueous solution, washed with ethanol, and treated with 50 mmol·L^{-1} $TiCl_4$ aqueous solution at 70°C for 30 min to make a good interfacial contact between TiO_2 layer and conductive glass substrate. A transparent adhesive tape was fixed on the four sides of conductive glass sheet to restrict the thickness and area of TiO_2 film. The above TiO_2 colloid was covered on the FTO glass plate by using a doctor scraping technique. Finally, the TiO_2 film was concreted by firing the FTO glass sheet at 450°C in air for 30 min. The process was repeated two times to form a thick TiO_2 film about 6–8 μm. After cooling down 80°C, the FTO glass was immersed in a 0.5 mmol·L^{-1} absolute ethanol solution of dye N719 for 24 h to absorb the dye adequately, then the dye-sensitized TiO_2 film was washed and dried in moisture-free air.

To reduce the combination of the electrons on the conductive glass with the holes in PCBM or P3HT, a barrier layer was covered on the conductive glass by following procedure [22]: Tetrabutyltitanate was dissolved in ethanol; acetylacetone as inhibitors was added to abate the hydrolysis reaction of tetrabutyltitanate. Under vigorous stirring, a nitric acid and acetic acid mixed water-ethanol solution was added, which lead to the hydrolysis of tetrabutyltitanate and a stable TiO_2 colloid was obtained. The molar ratio of $Ti(OBu)_4$:ETOH:H_2O:HNO_3:HAc was controlled at 1:8:2:0.2:0.5. Terpineol was added to adjust the viscosity of the colloid. The TiO_2 colloid was coated on the FTO glass plate using a doctor scraping technique. After sintering at 500°C for 30 min in air, the barrier layer with TiO_2 particle size of 5 nm and thickness of 1 μm was covered on the surface of the FTO plate. Then the same procedure was used to apply the dye-sensitized TiO_2 film on the plate.

2.3 Preparation of PEDOT:PSS/carbon electrode

A certain amount of PEDOT:PSS solution mixed DMSO which was polar solvent was added into a beaker together, and made the volume ratio of 4.5:1, then stirring at room temperature for 5 to 6 h to mix evenly of mixed solution and reach a certain viscosity; the original solution of

PEDOT:PSS/carbon got with adding a small amount of graphite powder and PVP by stirring for 12 h at room temperature. The PEDOT:PSS/carbon original solution 20 mL was stirred for 6 h at room temperature after adding a small amount of PEG-400, then PEDOT:PSS/carbon conductive solution prepared (shown in Fig. 1). Let PEDOT:PSS/carbon conductive solution coated on the FTO conductive glass under the infrared light irradiation scratching, made film thickness of 2–3 μm, and vacuum annealed at 80°C.

2.4 Fabrication of DSSC with PCBM/P3HT

PCBM and P3HT were mixed in a predetermined mass ratio and dissolved in 1, 2-dichlorobenzene solvent to form a conductive polymer solution with concentration of 15 mg·mL^{-1}, under stirring at 40°C for 24 h [3,25,26].

A DSSC was assembled by injecting a drop of the PCBM/P3HT solution into the aperture between the TiO_2 porous film electrode (anode electrode) and a PEDOT:PSS/carbon electrode. The two electrodes were clipped together, and a cyanoacrylate adhesive was used as a sealant to insulate from the air and water outside. Then the cell was placed overnight at room temperature to allow the PCBM/P3HT to penetrate into the aperture of the TiO_2 nonporous film completely. Thus, a TiO_2/dye/PCBM/P3HT/PEDOT:PSS/carbon solar cell that showed photoelectric performance stability for 10 days was assembled. The schematic diagram of the TiO_2/dye/PCBM/P3HT/PEDOT: PSS/carbon solar cell is shown in Fig. 1.

2.5 Measurements

Micromorphology of PEDOT:PSS/carbon electrode and TiO_2/PCBM/P3HT were observed by using JSM-6700F field emission scanning electron microscope (FESEM). Conductivity of PEDOT:PSS/carbon electrode was tested by RTS-9 model, 4-Point Probes Resistively Measurement System. Cyclic voltammetry (CV) of samples were measured in a three-electrode one-compartment cell with a PEDOT:PSS/carbon coated on FTO working electrode, Pt foil counter electrode and an Ag/AgCl reference electrode dipped in an acetonitrile solution of 10 mmol·L^{-1} LiI, 1 mmol·L^{-1} I_2, and 0.1 mol·L^{-1} $LiClO_4$. CV was performed using CHI660D electrochemical measurement system (scan condition: 40–200 mV·s^{-1}).

The photovoltaic test of the DSSCs was carried out by measuring photocurrent-photovoltage (*J-V*) character curves under irradiation of white light from a 100 mW·cm^{-2} (AM 1.5) with a solar simulator and (XQ-500W, Shanghai Photoelectricity Device Company, China) in ambient atmosphere and a computer controlled voltage current source-meter CHI660D electrochemical measurement system. The incident light intensity and the active cell area were 100 mW·cm^{-2} and 0.5 cm^2, respectively. The fill factor (*FF*) and the overall light-to-electrical energy conversion efficiency (η) of the solar cell were calculated according to the following equations [27]:

$$\eta(\%) = \frac{V_{\max} \times J_{\max}}{P_{\text{in}}} \times 100\% = \frac{V_{\text{OC}} \times J_{\text{SC}} \times FF}{P_{\text{in}}} \times 100\%, \quad (1)$$

$$FF = \frac{V_{\max} \times J_{\max}}{V_{\text{OC}} \times J_{\text{SC}}}, \quad (2)$$

where J_{SC} is the short-circuit current density (mA·cm^{-2}); V_{OC} is the open-circuit voltage (V), P_{in} is the incident light power, $J_{\max}$ (mA·cm^{-2}) and $V_{\max}$ (V) are the current density and voltage at the point of maximum power output in the *J-V* curves, respectively.

The spectral response of the solar cell was determined by measuring the wavelength dependence of the incident photon-to-current efficiency (IPCE) by focusing light from a xenon lamp through a monochromator (PXJ43B11, Japan) onto the cell. The IPCE was calculated according to the following equation [28]:

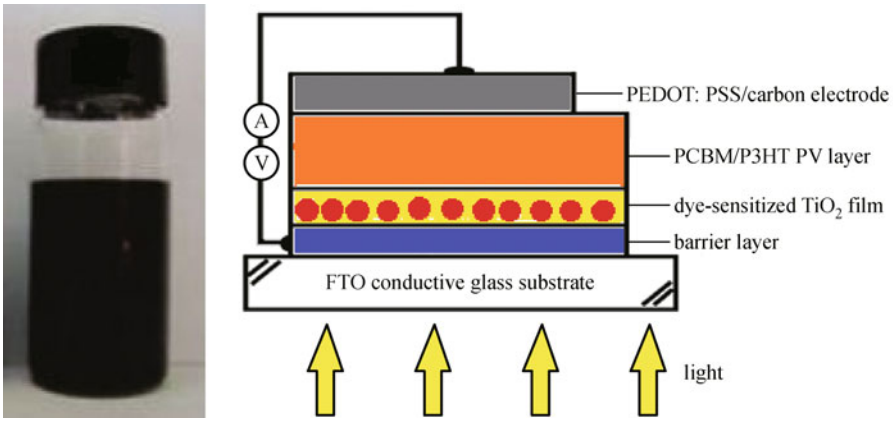

Fig. 1 A schematic diagram of the PEDOT:PSS/carbon conductive solution and TiO_2/dye/PCBM/P3HT/PEDOT:PSS/carbon solar cell

$$\mathrm{IPCE}(\lambda) = \frac{12400 \times J_{\mathrm{SC}}(\mathrm{mA \cdot cm^{-2}})}{\lambda(\mathrm{nm}) \times P_{\mathrm{in}}(\mathrm{mW \cdot cm^{-2}})}. \quad (3)$$

3 Results and discussion

3.1 Morphology and compositions of PEDOT:PSS/carbon electrode

Figure 2 shows the SEM image of PEDOT:PSS/carbon electrode. It was clear that the surface of electrode was smooth, and had smaller roughness before added graphite carbon (Fig. 2(a)). The surface of the electrode clearly exhibited an uplift structure when mixed graphite carbon (Figs. 2(b) and 2(c)), which increased the surface area of electrode and benefited the improvement of PCBM/P3HT solution penetration. On the other hand, the network structure of PEDOT:PSS helped to make uplift structure, which was good for improving the contact between anode and PEDOT:PSS/carbon electrode by trapping the PCBM/P3HT solution. In addition, for the SEM characterization, annealing could helpful to improve the smoothness, Figs. 2(b) and 2(c) were the impages of before and after annealing, we can see Fig. 2(c) was more smoother than Fig. 2(b). In short, annealing had impact on the smoothness of PEDOT:PSS/carbon electrode which affected by the transmission mechanism of PEDOT:PSS.

3.2 Electrochemical properties of PEDOT:PSS/carbon electrode

Cyclic voltammetrywas carried out by a Pt electrode or a PEDOT:PSS/carbon electrode as working electrode. A Pt coil as the counter electrode, and an Ag/Ag^{+} electrode as reference electrode. The electrolyte was the acetonitrile solution containing 0.1 $mol \cdot L^{-1}$ $LiClO_4$ as the supporting electrolyte and 10 $mmol \cdot L^{-1}$ LiI, 1 $mmol \cdot L^{-1}$ I_2 as the redox couple.

Figure 3 shows cyclic voltammograms of I_2/I^{-} system

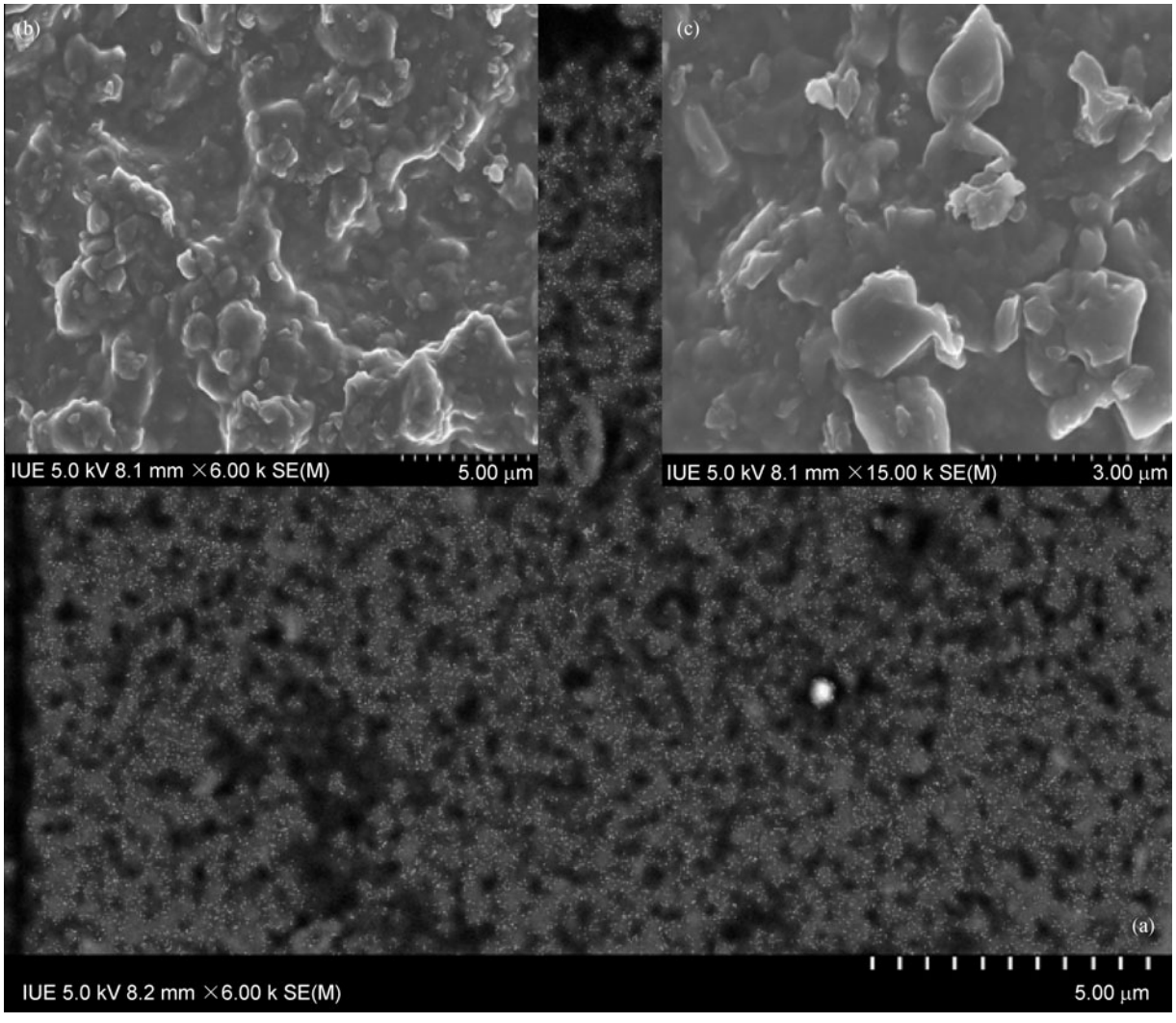

Fig. 2 SEM image of electrode (a) PEDOT:PSS coated on FTO glass (b) and (c) PEDOT: PSS/carbon electrode

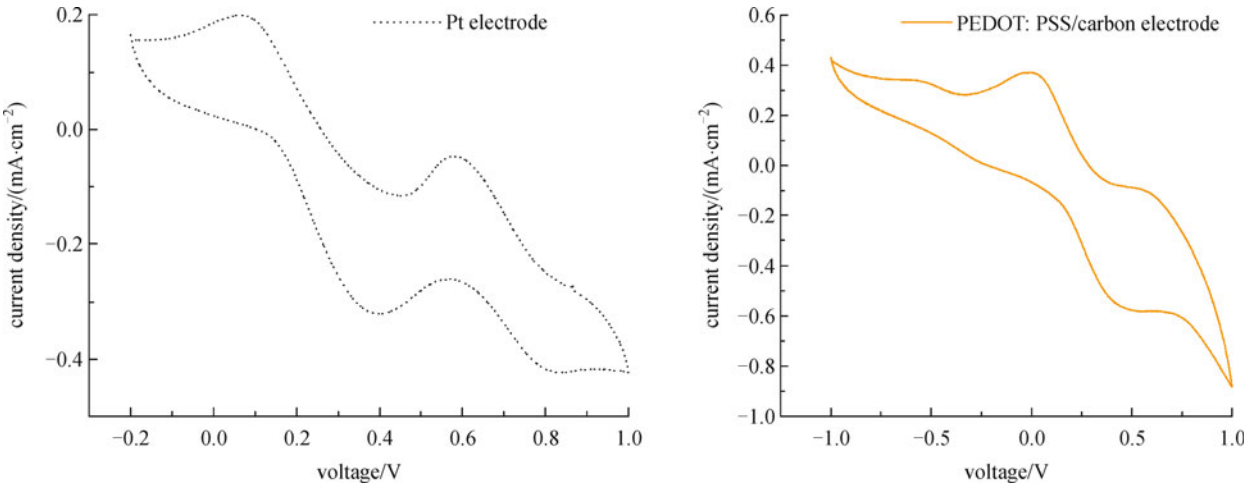

Fig. 3 Cyclic voltammograms for PEDOT:PSS/carbon electrode and Pt electrode at a scan rate of 50 mV·s^{-1} in 10 mmol·L^{-1} LiI, 1 mmol·L^{-1} I_2 acetonitrile solution containing 0.1 mol·L^{-1} $LiClO_4$ as the supporting electrolyte

for PEDOT:PSS/carbon electrode and Pt electrode at a scan rate of 50 mV·s^{-1} and $[I^-]/[I_2] = 10/1$. More negative pair is assigned to redox reaction (4) and more positive one is assigned to redox reaction (5) [29]:

$$I_3^- + 2e^- = 3I^- \quad (4)$$

$$3I_2 + 2e^- = 2I_3^- \quad (5)$$

In DSSC, electrons are injected to photooxidized dye from I^- ions in electrolyte (Eq. (5)), and the produced I_3^- are reduced on the counter electrode (Eq. (4)). Figure 3 shows a much higher current density of the I_3^- reduction peak for the PEDOT:PSS/carbon electrode than that for the Pt electrode. This suggests a faster reaction rate on the PEDOT:PSS/carbon electrode than that on the Pt electrode. In other words, the charge-transfer resistance (RCT) for the I_2/I^- redox reaction is smaller on the PEDOT:PSS/carbon electrode compared with Pt electrode under the same conditions [30]. And it can be observed clearly that the formal potential shifted more positive and a larger oxidation-reduction current density for the PEDOT:PSS/carbon electrode than Pt electrode in Fig. 3. Thus, the PEDOT:PSS/carbon electrode has a higher electrocatalytic activity in I_2/I^- redox reaction than that of Pt particle. On the other hand, the reduction peak in the left was not clear to that Pt electrode and the reason was also not clear until now [30], which had a little effect on the performance of DSSCs. Sum up, this indicates that PEDOT:PSS/carbon electrode can be used as an efficient electrocatalyst counter electrode in DSSCs.

Figure 4(a) shows consecutive cyclic voltammograms of I_2/I^- system for PEDOT:PSS/carbon electrode from + 1.0/ − 1.0 V (vs. Ag/AgCl) in the acetonitrile solution containing 0.1 mol·L^{-1} $LiClO_4$ as the supporting electrolyte and 10 mmol·L^{-1} LiI, 1 mmol·L^{-1} I_2 as the redox couple, and Pt foil is used as working electrode and the scan rate is 50 mV·s^{-1}. Two redox couples are observed. On successive scans, the peak currents density change with the change of scan rate. It indicates that the PEDOT:PSS/carbon was coated tightly on the FTO glass surface. Both redox peak currents show good linear relationship with the cycle times, as shown in Fig. 4(b). Therefore, it also indicates that the PEDOT:PSS/carbon film electrode is uniform and homogeneous [31].

3.3 Influence of the temperature on the conductivity properties of PEDOT:PSS/carbon electrode

The temperature and annealed environment had a great influence on the conductivity, resistivity and sheet resistance of PEDOT:PSS/carbon electrode as shown in Fig. 5, Tables 1 and 2. It is seen clearly the trend of conductivity, resistivity and sheet resistance change though these values are only approximation by four-electrode method. Series 1 (red color) were annealed in vacuum and series 2 (black color) were annealed in atmosphere shown in Fig. 5. It can be seen that the conductivities both increased with the heating temperature grew, then maximum values got 1.728 and 1.720 s·cm^{-1}, respectively, when the temperature at 80°C; the changed trend of resistivity and sheet resistance were opposite. Curve of series 1 was higher than those of series 2, that was because vacuum environment has less H_2O and O_2 than atmosphere, therefore, it had less impact on PEDOT:PSS/carbon electrode.

Maximum conductivity of vacuum annealed was higher than that in atmosphere annealed which mainly due to H_2O and O_2 under the vacuum had less impact on the electrode relative to the other series, but the heating time was longer. Because the absorption heat rate was quicker in the heating plate than that in the vacuum. On the other hand, the conductivity increased or decreased with increasing

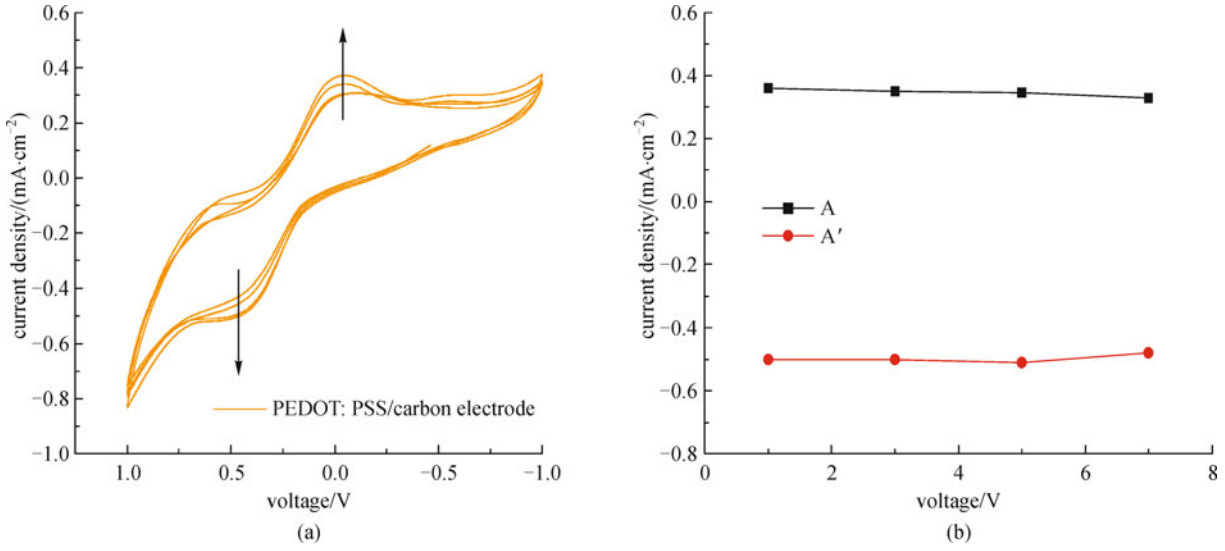

Fig. 4 (a) Consecutive four cyclic voltammograms of I_2/I^- system for PEDOT:PSS/carbon electrode in the acetonitrile solution containing 0.1 mol·L^{-1} $LiClO_4$ as the supporting electrolyte and 10 mmol·L^{-1} LiI, 1 mmol·L^{-1} I_2 as the redox couple, and Pt foil as working electrode and v = 50mV·s^{-1}; (b) relationship between the cycle times and the redox peak currents for PEDOT:PSS/carbon electrode

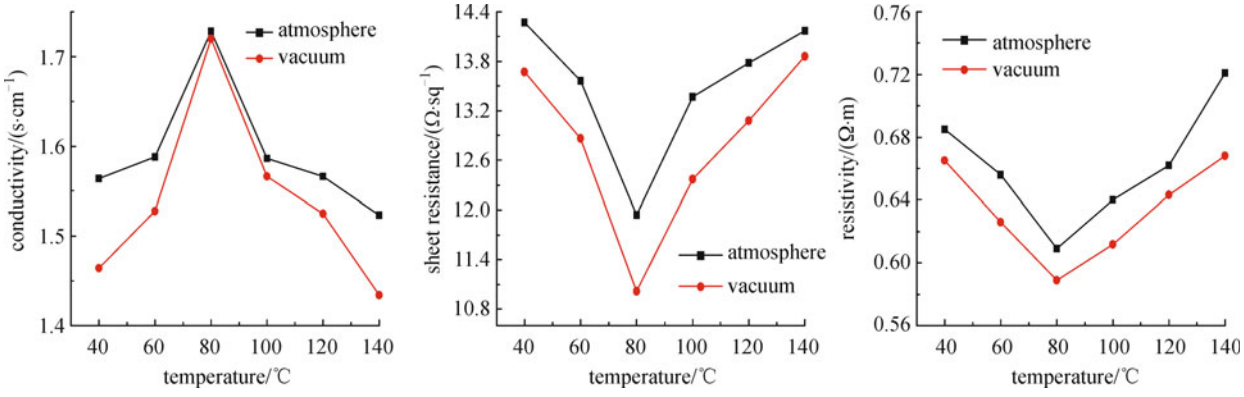

Fig. 5 Influence of the temperature and annealed environment on the conductivity, resistivity and sheet resistance of PEDOT:PSS/carbon electrode

Table 1 Influence of the temperature on the conductivity, resistivity and sheet resistance of PEDOT:PSS/carbon electrode in atmosphere environment annealed

temperature/°C	40	60	80	100	120	140
resistivity/(Ω·cm)	0.685	0.656	0.609	0.640	0.662	0.721
conductivity/(S·cm^{-1})	1.464	1.528	1.720	1.566	1.525	1.434
sheet resistance /(Ω·sq^{-1})	14.27	13.56	11.94	13.37	13.78	14.17

Table 2 Influence of temperature on the conductivity, resistivity and sheet resistance of PEDOT:PSS/carbon electrode in vacuum environment annealed

temperature/°C	40	60	80	100	120	140
resistivity/(Ω·cm)	0.665	0.626	0.589	0.612	0.643	0.668
conductivity/(S·cm^{-1})	1.564	1.588	1.728	1.586	1.566	1.523
sheet resistance/(Ω·sq^{-1})	13.67	12.86	11.02	12.37	13.08	13.86

temperature also affected by the transmission mechanism of PEDOT:PSS [32,33]. Particle size and the conductance between particles of PEDOT:PSS controlled the conductivity, at the right temperature, the connection among PSS and PEDOT particles were dissolved and soften, the number and height of the obstacles will be reduced, which will be more favorable toward the direction growth of crystallization of the polymer chains; thermal mass loss led to the conductivity decreased when continue to heat. In a conclusion, Fig. 5, Tables 1 and 2 indicated that annealed was good to improve the conductivity of PEDOT:PSS/carbon electrode.

3.4 Incident photon-to-current efficiency (IPCE)

Figure 6 compares the IPCEs of the DSSCs with PEDOT: PSS/carbon electrode and Pt electrode. These DSSCs have good photoelectric responses in the 350–360 nm (UV area) and 375–700 nm (visible-near infrared) ranges. The higher IPCEs in the UV range were mainly caused by the strong UV absorption of PCBM and TiO_2 film [34,35]. TiO_2 has an absorption peak around 350 nm that was related to the direct band gap photo-electron excitation of TiO_2 [35]. The higher IPCEs in the visible and near infrared areas were both caused by absorption of visible–near infrared light on the dye and visible light on the P3HT (such as the dip at 450 nm) [36]. From Fig. 6, it can be seen that the DSSC with PEDOT:PSS/carbon electrode has a higher IPCE value (17.3%) in the UV area (350–360 nm) than the DSSC with Pt electrode (12.1%). This indicated that the PEDOT: PSS/carbon electrode is promising replacement Pt electrode to photoelectric conversion through the light absorption of PCBM/P3HT.

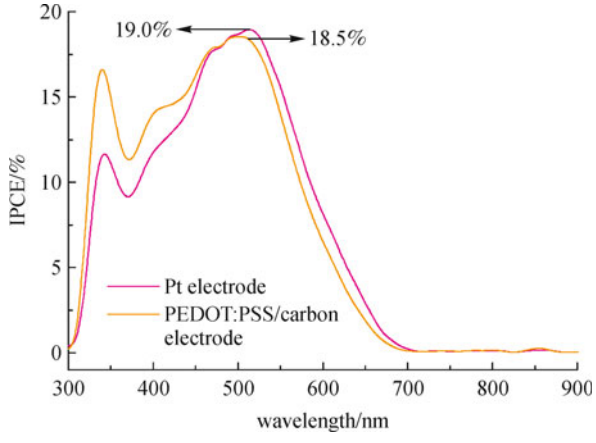

Fig. 6 IPCEs of DSSCs with PEDOT:PSS/carbon and Pt counter electrodes

3.5 Photovoltaic performance of DSSCs with PEDOT: PSS/carbon electrode

The photocurrent-voltage curves (Fig. 7) of the DSSCs

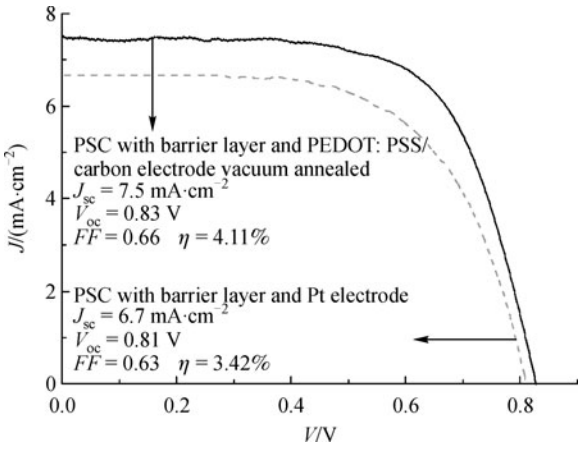

Fig. 7 Photocurrent-voltage characteristics of DSSCs (they both had barrier layer) with PEDOT:PSS/carbon (solid line) and Pt (dash line) counter electrodes under 100 mA·cm^{-2} light irradiation

with PEDOT: PSS/carbon counter electrode and Pt counter electrode were measured under irradiation of 100 mW·cm^{-2} which both had barrier layer. The photoelectric parameters of DSSCs such as short-circuit photocurrent density (J_{sc}), open circuit voltage (V_{oc}), fill factor (FF) and the overall energy conversion efficiency (η) was listed in Table 3. Comparing DSSCs with Pt electrode, all photoelectric parameters of the DSSCs with PEDOT:PSS/carbon electrodes were increased. The overall energy conversion efficiency of DSSCs with PEDOT: PSS/carbon electrode reached 4.11%, which was improved 20.2% compared with the DSSCs with Pt electrode.

Table 3 Photoelectric properties of DSSCs with PEDOT:PSS/carbon and Pt counter electrodes

	V_{oc}/V	J_{sc}/(mA·cm^{-2})	FF	η/%
Pt electrode	0.81	6.7	0.63	3.42
PEDOT:PSS/carbon electrode	0.83	7.5	0.66	4.11

The improvement of photoelectric performances for DSSCs based on PEDOT:PSS/carbon counter electrode mainly due to the following aspects. Firstly, the counter electrode with uplift structure engendered a large surface area on the electrode. The photoelectric performance of DSSCs can be improved with the increase of surface area of the electrode [37]. Secondly, the higher conductivity and smaller resistance increased the transmission capacity of electron and hole between PCBM/P3HT blend heterojunction and the PEDOT:PSS/carbon electrode. Thirdly, the higher electrocatalytic activity of PEDOT:PSS/carbon electrode resulted in the increasing of short-circuit photocurrent density, and blend heterojunction materials decided a higher open circuit voltage [3,4]. In addition, the polymer PEDOT: PSS as the material of electrode may be promoted to transmission of electron and hole by PCBM/P3HT blend heterojunction exciton splitting. The DSSCs

with a barrier layer could reduction in the recombination of the photo-induced electrons on the conductive glass substrate with free charge carriers, and increased in the number of photoelectrons from the external circuit reaching the photocathode and an reduction in the dark current which helped to improve photocurrent density. Therefore, the DSSCs with PEDOT:PSS/carbon electrode has predominant photoelectric performance.

4 Conclusions

In summary, PEDOT:PSS/carbon conductive paste was prepared and coated on a conducting FTO glass to construct PEDOT:PSS/carbon counter electrode used in polymer heterojunction DSSCs. The surface morphology of PEDOT:PSS/carbon electrode we can observed the uplift structure by SEM, which provided a larger surface area for electrode; there was good electrochemical properties at 80°C in vacuum annealed, such as higher conductivity, smaller sheet resistance, better redox properties and photoelectric properties, which were observed respectively using four-probe tester and CHI660D electrochemical measurement system. The overall energy conversion efficiency of DSSCs with PEDOT:PSS/carbon counter electrode reached 4.11% under irradiation of a simulated solar light with a intensity of 100 $mW \cdot cm^{-1}$ (AM 1.5), which is higher (20%) than that of the DSSCs with Pt counter electrode (3.42%). The IPCEs of DSSCs with PEDOT:PSS/carbon counter electrode was higher 43.0% in the 350–360 nm (UV area) than that of Pt electrode. The excellent photoelectric properties, simple preparation procedure and inexpensive cost allow the PEDOT:PSS/carbon electrode to be a credible alternative used in DSSCs.

Acknowledgements This work was supported by the National High Technology Research and Development Program of China (No. 2009AA03Z217), and the National Natural Science Foundation of China (Grant Nos. 90922028, 50842027, 51002053).

References

1. O'Regan B, Gratzel M. A low-cost, high-efficiency solar cell based on dye-sensitized colloidal TiO_2 films. Nature, 1991, 353(6346): 737–740
2. Yu G, Gao J, Hummelen J C, Wudl F, Heeger A J. Polymer photovoltaic cells: enhanced efficiencies via a network of internal donor-acceptor heterojunctions. Science, 1995, 270(5243): 1789–1791
3. Wu J H, Yue G T, Xiao Y M, Ye H F, Lin J M, Huang M L. Application of a polymer heterojunction in dye-sensitized solar cells. Electrochimica Acta, 2010, 55(20): 5798–5802
4. Grätzel M. Solar energy conversion by dye-sensitized photovoltaic cells. Inorganic Chemistry, 2005, 44(20): 6841–6851
5. Wu J, Lan Z, Hao S, Li P, Lin J, Huang M, Fang L, Huang Y. Progress on the electrolytes for dye-sensitized solar cells. Pure and Applied Chemistry, 2008, 80(11): 2241–2258
6. Wu J, Hao S, Lan Z, Lin J, Huang M, Huang Y, Li P, Yin S, Sato T. An all-solid-state dye-sensitized solar cell-based poly(*N*-alkyl-4-vinyl-pyridine iodide) electrolyte with efficiency of 5.64%. Journal of the American Chemical Society, 2008, 130(35): 11568–11569
7. Bach U, Lupo D, Comte P, Moser J E, Weissortel F, Salbeck J, Grätzel M. Solid-state dye-sensitized mesoporous TiO_2 solar cells with high photon-to-electron conversion efficiencies. Nature, 1998, 395(6702): 583–585
8. Grätzel M. Photoelectrochemical cells. Nature, 2001, 414(6861): 338–344
9. Wu J, Lan Z, Lin J M, Huang M L, Hao S C, Sato T, Yin S. A novel thermosetting gel electrolyte for stable quasi-solid-state dye-sensitized solar cells. Advanced Materials (Deerfield Beach, Fla.), 2007, 19(22): 4006–4011
10. Peter L M. Dye-sensitized nanocrystalline solar cells. Physical Chemistry Chemical Physics, 2007, 9(21): 2630–2642
11. Papageorgiou N. Counter-electrode function in nanocrystalline photoelectrochemical cell configurations. Coordination Chemistry Reviews, 2004, 248(13–14): 1421–1446
12. Jeon S S, Kim C, Ko J, Im S S. Spherical polypyrrole nanoparticles as a highly efficient counter electrode for dye-sensitized solar cells. Journal of Materials Chemistry, 2011, 21(22): 8146–8151
13. Halme J, Toivola M, Tolvanen A, Lund P. Charge transfer resistance of spray deposited and compressed counter electrodes for dye-sensitized nanoparticle solar cells on plastic substrates. Solar Energy Materials and Solar Cells, 2006, 90(7–8): 872–886
14. Zhu H W, Zeng H F, Subramanian V, Masarapu C, Hung K H, Wei B. Anthocyanin-sensitized solar cells using carbon nanotube films as counter electrodes. Nanotechnology, 2008, 19(46): 465204
15. Lee W J, Ramasamy E, Lee D Y, Song J S. Efficient dye-sensitized solar cells with catalytic multiwall carbon nanotube counter electrodes. ACS Applied Materials & Interfaces, 2009, 1(6): 1145–1149
16. Ramasamy E, Lee W J, Lee D Y, Song J S. Spray coated multi-wall carbon nano-tube counter electrode for tri-iodide (I_3^-) reduction in dye-sensitized solar cells. Electrochemistry Communications, 2008, 10(7): 1087–1089
17. Kay A, Grätzel M. Low cost photovoltaic modules based on dye sensitized nanocrystalline titanium dioxide and carbon powder. Solar Energy Materials and Solar Cells, 1996, 44(1): 99–117
18. Li G R, Wang F, Jiang Q W, Gao X P, Shen P W. Carbon nanotubes with titanium nitride as a low-cost counter-electrode material for dye-sensitized solar cells. Angewandte Chemie International Edition, 2010, 49(21): 3653–3656
19. Najafi E, Kim J Y, Han S H, Shin K. UV-ozone treatment of multi-walled carbon nanotubes for enhanced organic solvent dispersion. Colloid Surf. A, 2006, 284-285: 373–378
20. Kim K K, Yoon S M, Choi J Y, Lee J, Kim B K, Kim J M, Lee J H, Paik U, Park M H, Yang C W, An K H, Chung Y, Lee Y H. Design of dispersants for the dispersion of carbon nanotubes in an organic solvent. Advanced Functional Materials, 2007, 17(11): 1775–1783
21. Wu T M, Lin Y W, Liao C S. Preparation and characterization of

polyaniline/multi-walled carbon nanotube composites. Carbon, 2005, 43(4): 734–740

22. Yun D J, Hong K, Kim S, Yun W M, Jang J Y, Kwon W S, Park C E, Rhee S W. Multiwall carbon nanotube and poly(3,4-ethylenedioxythiophene): polystyrene sulfonate (PEDOT:PSS) composite films for transistor and inverter devices. ACS Applied Materials & Interfaces, 2011, 3(1): 43–49
23. Jonsson S K M, Birgerson J, Crispin X, Greczynski G, Osikowicz W, Gon A W D, Salaneck W R, Fahlman M. The effects of solvents on the morphology and sheet resistance in poly (3, 4-ethylenedioxythiophene)-polystyrenesulfonic acid (PEDOT-PSS) films. Synthetic Metals, 2003, 139(1): 1–10
24. Groenendaal L, Jonas F, Feitag D, Pielartzik H, Reynolds J R. Poly (3, 4-ethylenedioxythiophene) and its derivatives: past, present, and future. Advanced Materials (Deerfield Beach, Fla.), 2000, (12): 482
25. Hwang J, Amy F, Kahn A. Spectroscopic study on sputtered PEDOT· PSS: role of surface PSS layer. Organic Electronics, 2006, 7(5): 387–396
26. Zhou E, Tan Z, Huo L, He Y, Yang C, Li Y. Effect of branched conjugation structure on the optical, electrochemical, hole mobility, and photovoltaic properties of polythiophenes. Journal of Physical Chemistry B, 2006, 110(51): 26062–26067
27. Grätzel M. Photoelectrochemical cells. Nature, 2001, 414(6861): 338–344
28. Renouard T, Fallahpour R A, Nazeeruddin M K, Humphry-Baker R, Gorelsky S I, Lever A B, Grätzel M. Novel ruthenium sensitizers containing functionalized hybrid tetradentate ligands: synthesis, characterization, and INDO/S analysis. Inorganic Chemistry, 2002, 41(2): 367–378
29. Popov A I, Geske D H. Voltammetric evaluation of the stability of trichloride, tribromide, and triiodide ions in nitromethane, acetone, and acetonitrile. Journal of the American Chemical Society, 1958, 80(6): 1340–1352
30. Imoto K, Takahashi K, Yamaguchi T, Komura T, Nakamura J, Murata K. High-performance carbon counter electrode for dye-sensitized solar cells. Solar Energy Materials and Solar Cells, 2003, 79(4): 459–469
31. Guo H, Li Y, Fan L, Wu X, Guo M. Voltammetric behavior study of folic acid at phosphomolybdic-polypyrrole film modified electrode. Electrochimica Acta, 2006, 51(28): 6230–6237
32. Huang J, Miller P F, de Mello J C, de Mello A J, Bradley D D C. Influence of thermal treatment on the conductivity and morphology of PEDOT/PSS films. Synthetic Metals, 2003, 139(3): 569–572
33. Aasmundtveit K E, Samuelsen E J, Pettersson L A A, Inganäs O, Johansson T, Feidenhans'l R. Structure of thin films of poly (3, 4-ethylenedioxythiophene). Synthetic Metals, 1999, 101(1–3): 561–564
34. Al-Ibrahim M, Ambacher O, Sensfuss S, Gobsch G. Effects of solvent and annealing on the improved performance of solar cells based on poly (3-hexylthiophene): fullerene. Applied Physics Letters, 2005, 86(20): 201120
35. Senadeera G, Kitamura T, Wada Y, Yanagida S. Photosensitization of nanocrystalline TiO_2 films by a polymer with two carboxylic groups, poly (3-thiophenemalonic acid). Solar Energy Materials and Solar Cells, 2005, 88(3): 315–322
36. Lee J, Kim W, Lee H, Shin W, Jin S, Lee W, Kim M. Preparations and photovoltaic properties of dye–sensitized solar cells using thiophene–based copolymers as polymer electrolytes. Polymers for Advanced Technologies, 2006, 17(9–10): 709–714
37. Thampi K R, Kiwi J, Grätzel M. Methanation and photo-methanation of carbon dioxide at room temperature and atmospheric pressure. Nature, 1987, 327(6122): 506–508